

# Effect of Inhibition of Spinal Cord Glutamate Transporters on Inflammatory Pain Induced by Formalin and Complete Freund's Adjuvant

Myron Yaster, M.D.,\* Xiaowei Guan, M.D., Ph.D.,† Ronald S. Petralia, Ph.D.,‡  
Jeffery D. Rothstein, M.D.,§ Wei Lu, Ph.D.,|| Yuan-Xiang Tao, M.D., Ph.D.#

## ABSTRACT

**Background:** Spinal cord glutamate transporters clear synaptically released glutamate and maintain normal sensory transmission. However, their ultrastructural localization is unknown. Moreover, whether and how they participate in inflammatory pain has not been carefully studied.

**Methods:** Immunogold labeling with electron microscopy was carried out to characterize synaptic and nonsynaptic localization of glutamate transporters in the superficial dorsal

### What We Already Know about This Topic

- Glutamate is a major excitatory neurotransmitter in the dorsal horn of the spinal cord and is critical for pain transmission.
- Glutamate transporters terminate activity by glutamate through reuptake into neurons and glia.

### What This Article Tells Us That Is New

- Spinally injected glutamate transport inhibitors are paradoxically antihyperalgesic in two pain models.
- Spinally injected glutamate transport inhibitors cause antihyperalgesic effects through presynaptic inhibitory metabotropic glutamate receptor activation.

\* Professor, Department of Anesthesiology and Critical Care Medicine, § Professor, Department of Neurology and Neuroscience, Johns Hopkins University School of Medicine, Baltimore, Maryland. † Trainee, Department of Anesthesiology and Critical Care Medicine, Johns Hopkins University School of Medicine, and Instructor, Department of Anatomy, Nanjing Medical University School of Basic Medical Sciences, Jiangsu Province, China. ‡ Staff Scientist, Laboratory of Neurochemistry, National Institute of Deafness and Other Communication Disorders, National Institutes of Health, Bethesda, Maryland. || Professor, Department of Neurobiology, Nanjing Medical University School of Basic Medical Sciences. # Associate Professor, Department of Anesthesiology and Critical Care Medicine, Johns Hopkins University School of Medicine, and Guest Professor, Departments of Anatomy and Neurobiology, Nanjing Medical University School of Basic Medical Sciences.

Received from the Department of Anesthesiology and Critical Care Medicine, Johns Hopkins University School of Medicine, Baltimore, Maryland. Submitted for publication July 8, 2010. Accepted for publication October 12, 2010. Supported by the National Institutes of Health (Bethesda, Maryland) Grant no. R01NS058886, the National Natural Science Foundation of China (Beijing) Grant no. 30828015, the Blaustein Pain Research Fund (Baltimore, Maryland), the Mr. David Koch and Patrick C. Walsh Prostate Cancer Research Fund (Baltimore, Maryland), and the Intramural Research Program of the National Institute of Deafness and Other Communication Disorders (Bethesda, Maryland). This is a work prepared by U.S. government-employed personnel. No claim is made to original works by U.S. government employees. The work is the opinion of the authors alone and not of the U.S. government. Drs. Yaster and Guan contributed equally to this work.

Address correspondence to Dr. Tao: Department of Anesthesiology and Critical Care Medicine, Johns Hopkins University School of Medicine, 1721 E. Madison St., 370 Ross, Baltimore, Maryland 21205. ytao1@jhmi.edu. Information on purchasing reprints may be found at [www.anesthesiology.org](http://www.anesthesiology.org) or on the masthead page at the beginning of this issue. ANESTHESIOLOGY's articles are made freely accessible to all readers, for personal use only, 6 months from the cover date of the issue.

Copyright © 2011, the American Society of Anesthesiologists, Inc. Lippincott Williams & Wilkins. Anesthesiology 2011; 114: 412-23

horn. Their expression and uptake activity after formalin- and complete Freund's adjuvant (CFA)-induced inflammation were evaluated by Western blot analysis and glutamate uptake assay. Effects of intrathecal glutamate transporter activator (R)-(-)-5-methyl-1-nicotinoyl-2-pyrazoline and inhibitors (DL-threo- $\beta$ -benzyloxyaspartate [TBOA], dihydrokainate, and DL-threo- $\beta$ -hydroxyaspartate), or TBOA plus group III metabotropic glutamate receptor antagonist (RS)- $\alpha$ -methylserine-O-phosphate, on formalin- and CFA-induced inflammatory pain were examined.

**Results:** In the superficial dorsal horn, excitatory amino acid carrier 1 is localized in presynaptic membrane, postsynaptic membrane, and axonal and dendritic membranes at nonsynaptic sites, whereas glutamate transporter-1 and glutamate/aspartate transporter are prominent in glial membranes. Although expression of these three spinal glutamate transporters was not altered 1 h after formalin injection or 6 h after CFA injection, glutamate uptake activity was decreased at these time points. Intrathecal (R)-(-)-5-methyl-1-nicotinoyl-2-pyrazoline had no effect on formalin-induced pain behaviors. In contrast, intrathecal TBOA, dihydrokainate, and DL-threo- $\beta$ -hydroxyaspartate reduced formalin-evoked pain behaviors in the second phase. Intrathecal TBOA also attenuated CFA-induced thermal hyperalgesia at 6 h after CFA injection. The antinociceptive effects of TBOA were blocked by coadministration of (RS)- $\alpha$ -methylserine-O-phosphate.

**Conclusion:** Our findings suggest that spinal glutamate transporter inhibition relieves inflammatory pain through activation of inhibitory presynaptic group III metabotropic glutamate receptors.

**T**HE AMINO acid glutamate is the major excitatory neurotransmitter in the spinal cord dorsal horn and participates in the induction and maintenance of pain hypersensitivity after tissue injury and inflammation.<sup>1,2</sup> In the dorsal horn, glutamate is released synaptically by primary afferent terminals, descending terminals from supraspinal regions, and excitatory interneurons.<sup>3</sup> Activation of the group III metabotropic glutamate receptors (mGluRs) in the primary afferent terminals inhibits the release of synaptic glutamate in the superficial dorsal horn.<sup>4,5</sup> The synaptically released glutamate is also rapidly taken up through glutamate transporters to ensure high-fidelity sensory transmission, limiting nonsynaptic neuronal excitation and hyperactivity and also preventing excitatory toxicity.<sup>6</sup> However, little is known about the regulation of synaptically released glutamate by spinal glutamate transporters under inflammatory pain conditions.

To date, five glutamate transporters have been cloned and characterized from animal and human tissues, including glutamate/aspartate transporter (GLAST), glutamate transporter-1 (GLT-1), excitatory amino acid carrier 1 (EAAC1), excitatory amino-acid transporter 4, and excitatory amino-acid transporter 5.<sup>2</sup> Each has a distinct cellular and regional localization. EAAC1 is localized in neuronal cells of the nervous system, whereas GLAST and GLT-1 are predominantly present in glial cells throughout the central nervous system.<sup>7,8</sup> Excitatory amino-acid transporter 4 has properties of a ligand-gated chloride channel and is localized mainly in cerebellar Purkinje cells.<sup>9</sup> Excitatory amino-acid transporter 5 is retina-specific.<sup>10</sup> We and others<sup>6,8,11–13</sup> have shown that EAAC1, GLAST, and GLT-1 are expressed in the spinal cord whereas EAAC1 is also expressed in dorsal root ganglion (DRG). However, their synaptic and nonsynaptic localization and distribution in the dorsal horn have not been carefully studied.

Spinal glutamate transporters play a role in normal sensory transmission and pathologic pain states. Spinal glutamate transporter inhibition produces hyperactivity of dorsal horn neurons, spontaneous nociceptive behavior, and thermal and mechanical hypersensitivity in normal rats,<sup>14,15</sup> suggesting that glutamate uptake through spinal glutamate transporters is required for maintaining normal sensory transmission. Unexpectedly, in pathologic pain states, inhibition of spinal glutamate transporter activity produces antinociceptive effects. For example, spinal glutamate transporter inhibition attenuated the induction of allodynia induced by intrathecal prostaglandin E<sub>2</sub>, prostaglandin F<sub>2 $\alpha$</sub> , and *N*-methyl-D-aspartic acid.<sup>16</sup> In addition, inhibition or transient knockdown of spinal GLT-1 and GLAST led to a significant reduction of nociceptive behavior in the formalin model.<sup>12,17</sup> However, knockdown of spinal GLAST did not affect zymosan-induced inflammatory pain.<sup>12</sup> Moreover, intrathecal administration of a glutamate transporter activator, riluzole, reversed neuropathic pain behavior.<sup>13</sup> Thus, whether and how spinal glutamate transporters participate in pathologic pain is still not completely understood.

In the current study, we first characterized synaptic and nonsynaptic localization and distribution of GLAST, GLT-1, and EAAC1 in the superficial dorsal horn of the spinal cord. We then examined whether regulating spinal glutamate transporter uptake activity affects inflammatory pain induced by intraplantar injection of formalin or complete Freund's adjuvant (CFA). Finally, we investigated whether inhibitory presynaptic group III mGluRs are involved in spinal glutamate transporter function in inflammatory pain.

## Materials and Methods

### Animal Preparation

Male Sprague-Dawley rats (250–300 g, Harlan Bioproducts for Science, Inc., Indianapolis, IN) were housed individually in cages on a standard 12-h light-dark cycle. Water and food were available *ad libitum* until rats were transported to the laboratory, approximately 1 h before the experiments. Experiments were carried out with the approval of the Animal Care and Use Committee at The Johns Hopkins University (Baltimore, Maryland) and were consistent with the ethical guidelines of the National Institutes of Health and the International Association for the Study of Pain. All efforts were made to minimize the number of animals used and their suffering.

Rats were anesthetized with isoflurane and implanted with an intrathecal catheter. A polyethylene-10 catheter was inserted into the subarachnoid space at the rostral level of the spinal cord lumbar enlargement through an incision at the atlanto-occipital membrane according to methods described previously.<sup>14,18,19</sup> The animals were allowed to recover for 1 week before being used experimentally. Rats showing postoperative neurologic deficits were discarded from the study. After the experiments, the location of the intrathecal catheter was confirmed and lumbar enlargement segments were harvested for histochemical staining as described.<sup>14</sup> Animal behavioral tests, including formalin testing and CFA-induced thermal testing, were carried out by one experimenter who was blinded to group assignments.

### Experimental Drugs

CFA and formalin were purchased from Sigma-Aldrich (St. Louis, MO). (R)-(-)-5-methyl-1-nicotinoyl-2-pyrazoline (MS-153), a glutamate transporter activator, was a gift from the Life Science Laboratory at Mitsui Chemical, Inc. (Chiba, Japan). Three glutamate transporter inhibitors, DL-threo- $\beta$ -benzyloxypartate (TBOA), DL-threo- $\beta$ -hydroxyaspartate (DL-THA), and dihydrokainate, and a selective group III mGluR antagonist, (RS)- $\alpha$ -methylserine-O-phosphate (MSOP), were purchased from Tocris Bioscience (Ellisville, MO). All drugs were dissolved in physiologic saline, 0.9%. Doses used were based on data from previous studies<sup>14</sup> and our pilot work.

### Assessment of Formalin-induced Pain Behaviors

Rats were placed individually in an open plexiglass chamber (34 × 30 × 30 cm) for 1 h before experimental sessions. To

examine whether altering spinal glutamate transporter uptake activity affected formalin-induced pain behaviors, we intrathecally injected saline (control, 10  $\mu$ l; n = 10), MS-153 (10, 100, or 1,000  $\mu$ g/10  $\mu$ l; n = 5 each group), DL-THA (1.5, 7.5, or 15  $\mu$ g/10  $\mu$ l; n = 6 each group), dihydrokainate (2, 10, or 20  $\mu$ g/10  $\mu$ l; n = 7 each group), or TBOA (1, 5, or 10  $\mu$ g/10  $\mu$ l; n = 10 each group) followed by 10  $\mu$ l of saline to flush the catheter. Ten minutes later, the experimenter injected 100  $\mu$ l formalin, 2%, into the plantar side of one hind paw and immediately placed the rat into a transparent cage to count the number of paw flinches and shakes in the next 60 min.<sup>20,21</sup> The observational session was divided into two phases: 0–10 min and 10–60 min. The mean number of flinches and shakes for each phase of the observational session was calculated for each treatment group.

To examine the role of group III mGluRs in the antinociceptive effect produced by intrathecal TBOA in the formalin model, we intrathecally injected the rats with saline (10  $\mu$ l; n = 5), MSOP (10  $\mu$ g/10  $\mu$ l; n = 5), TBOA (10  $\mu$ g/10  $\mu$ l; n = 5), or MSOP plus TBOA (n = 5). Ten minutes later, 100  $\mu$ l formalin, 2%, was injected into the plantar side of a hind paw and formalin-induced pain behaviors were assessed.

### Assessment of CFA-induced Thermal Pain Hypersensitivity

To induce persistent inflammatory pain, CFA (100  $\mu$ l, 1 mg/ml *Mycobacterium tuberculosis*) solution was injected into the plantar side of one hind paw. Our previous studies showed that CFA-induced thermal pain hypersensitivity reaches a peak level at 6 h and persists for at least 24 h postinjection.<sup>22</sup> We chose these two time points for the pharmacologic and behavioral studies. At 6 h and 24 h after CFA injection, we intrathecally injected saline (10  $\mu$ l; n = 5/time point) or TBOA (1, 5, or 10  $\mu$ g/10  $\mu$ l; n = 5 each group and time point) followed by 10  $\mu$ l of saline to flush the catheter. Thermal testing was carried out 1 day before CFA injection (baseline) and at 20 min after saline or TBOA administration. Paw withdrawal response to thermal stimulation was measured as described previously.<sup>14,18,19</sup> In brief, each rat was placed in a Plexiglas chamber on a glass plate above a light box. A beam of radiant heat from the apparatus (model 336T; IITC Life Science, Inc., Woodland Hills, CA) was applied through a hole in the light box to the middle of the plantar surface of each hind paw through the glass plate. When the rat lifted its foot the light beam automatically shut off. The length of time between the start of the light beam and the foot lift was defined as the paw withdrawal latency. Each trial was repeated five times at 5-min intervals for each side. A cut-off time of 20 s was used to avoid tissue damage to the paw.

To examine the role of group III mGluRs in the antinociceptive effect produced by intrathecal TBOA in the CFA model, we intrathecally injected the rats with saline (10  $\mu$ l; n = 5), MSOP (10  $\mu$ g/10  $\mu$ l; n = 5), TBOA (10  $\mu$ g/10  $\mu$ l;

n = 5), or MSOP plus TBOA (n = 5) at 6 h post-CFA and then measured paw withdrawal latencies.

### Locomotor Function Testing

To examine whether the glutamate transporter inhibitors used in behavioral testing affected locomotor function, three reflexes (placing, grasping, and righting) were tested as described previously.<sup>14,18,21,22</sup> In brief, naive animals received a 10- $\mu$ l intrathecal injection of saline (10  $\mu$ l; n = 5), DL-THA (15  $\mu$ g/10  $\mu$ l; n = 5), dihydrokainate (20  $\mu$ g/10  $\mu$ l; n = 5), or TBOA (10  $\mu$ g/10  $\mu$ l; n = 5). Twenty minutes later, an experimenter blind to drug treatment tested the rats for placing, grasping, and righting reflexes as published previously.<sup>14,18,21,22</sup> Scores for each reflex were based on counts of each normal reflex exhibited in five trials. In addition, the rats' general behaviors, including spontaneous activity (*e.g.*, walking and running), were observed.

### Total RNA Preparation and Reverse Transcriptase–Polymerase Chain Reaction

Total RNA from the spinal cord, DRG, hippocampus, and cortex of rats (n = 2) was extracted by the TRIzol<sup>®</sup> method (Invitrogen, Carlsbad, CA), precipitated with isopropanol, and treated with DNase I (New England Biolabs, Inc., Ipswich, MA). The quality and quantity of RNA samples were by spectrophotometer (NanoDrop 1000 UV-VIS; Thermo Fisher Scientific, Inc., Wilmington, DE). First-strand complementary DNA was synthesized from total RNA (Omniscript RT Kit; QIAGEN, Valencia, CA). Template (1  $\mu$ l) was amplified by polymerase chain reaction (PCR) with Platinum Taq DNA polymerase (1 unit) in 20  $\mu$ l of total reaction volume containing 0.5  $\mu$ mol of each specific PCR primer. The primer sequences were chosen from the conserved part of the coding region for GLAST [5'–GAAAGATAAAATATGCAAAAAGCAAC–3' (forward) and 5'–GTTGCTTTTTTGTGCATATTTTATC–TTTC–3' (reverse)] and for GLT-1 [5'–ATCAACCGAG–GGTGTGCCAACAATAT–3' (forward) and 5'–ATATT–GTTGGCACCCTCGGTTGAT–3' (reverse)]. As a loading control,  $\beta$ -actin complementary DNA was also amplified with primer sequences 5'–TCACCCACACTGTGCCCATC–TACGA–3' (forward) and 5'–GGATGCCACAGGATTC–CATACCCA–3' (reverse). PCR amplification was carried out for 30 cycles consisting of 20 s at 94°C, 20 s at 55°C, and 30 s at 72°C. After amplification, the products were separated on a 1.2% agarose gel containing ethidium bromide, 0.025%. Bands were visualized under ultraviolet illumination and gels were photographed (BioDoc-It Imaging System; UVP, LLC, Upland, CA).

### Western Blot Analysis

Rats (N = 20; formalin and saline [n = 10] *vs.* CFA and saline [n = 10]) were sacrificed by decapitation. Dorsal and ventral tissues of the lumbar enlargement segments and DRG were dissected, rapidly frozen in liquid nitrogen, and stored at –80°C. Soluble proteins were prepared according



to procedures described previously.<sup>18–21</sup> In brief, frozen tissues were homogenized in homogenization buffer (50 mM Tris-hydrochloric acid, 0.1 mM EDTA, 0.1 mM EGTA, 1 mM phenylmethylsulfonyl fluoride, 1  $\mu$ M leupeptin, 2  $\mu$ M pepstatin A). At 4°C, crude homogenate was centrifuged for 15 min at 3,000g. Supernatant was collected, and the pellet (nuclei and debris fraction) discarded. After protein concentration was measured, samples were heated for 5 min at 98°C and loaded onto 4% stacking/7.5% separating sodium dodecyl sulfate-polyacrylamide gels for protein separation. Protein was electrophoretically transferred onto a nitrocellulose membrane. The membrane was blocked with 3% nonfat dry milk and subsequently incubated for 2 h with polyclonal rabbit primary antibody for GLAST (0.05  $\mu$ g/ml), EAAC1 (0.06  $\mu$ g/ml), or GLT-1 (0.05  $\mu$ g/ml). All antibodies were provided (September 10, 2005), by Jeffery D. Rothstein, M.D., Ph.D. (Professor, Department of Neurology, Johns Hopkins University, Baltimore, Maryland). Their specificity and selectivity have been reported previously.<sup>8,11,23–25</sup>  $\beta$ -actin (monoclonal mouse primary antibody against  $\beta$ -actin, 0.2  $\mu$ g/ml; Santa Cruz Biotechnology, Inc., Santa Cruz, CA) was used as a loading control. The proteins were detected by horseradish peroxidase-conjugated anti-rabbit or anti-mouse secondary antibodies and visualized with chemiluminescence reagents (ECL Kit; Amersham Pharmacia Biotech, Piscataway, NJ) and exposure to film. The intensity of blots was quantified with densitometry.

### Immunohistochemistry

Rats (n = 3) were deeply anesthetized with isoflurane and perfused with 4% paraformaldehyde in phosphate buffer (0.1 M, pH 7.4). Spinal cord L4 and L5 segments and DRG were harvested, postfixed in the same fixative solution for 2–4 h, cryoprotected by immersion in 30% sucrose overnight at 4°C, and frozen-sectioned at 25  $\mu$ m. The sections were blocked for 1 h at 37°C in 0.01 M phosphate-buffered saline containing 10% normal goat serum plus 0.3% Triton X-100. Sections were incubated in primary rabbit antibody for GLAST (1:500), EAAC1 (1:1,000), or GLT-1 (1:1,000) for 48 h at 4°C. Sections were finally incubated in biotinylated goat anti-rabbit immunoglobulin G (1:200; Vector Laboratories, Burlingame, CA) for 1 h at 37°C followed by avidin-biotin-peroxidase complex (1:100; Vector Laboratories) for 1 h at 37°C. The immune reaction product was visualized by catalysis of 3,3'-diaminobenzidine by horseradish peroxidase in the presence of 0.01% H<sub>2</sub>O<sub>2</sub>.

### Postembedding Immunogold Labeling and Electron Microscopy

Postembedding immunogold labeling was carried out as described previously.<sup>19,26</sup> In brief, animals (n = 2) were perfused transcardially with 4% paraformaldehyde and 0.5% glutaraldehyde. Cryoprotected sections from the L5 superficial dorsal horn were frozen in a cryopreparation chamber

(Leica Microsystems AG, Wetzlar, Germany) and freeze-substituted into Lowicryl HM-20 in a Leica automatic freeze substitution instrument. Ultrathin sections were labeled with polyclonal rabbit antibody for EAAC1, GLAST, and GLT-1. Sections were double labeled with polyclonal rabbit antibody for EAAC1 and monoclonal mouse antibody for calcitonin gene-related peptide. Control experiments for specificity and selectivity of these antibodies were carried out as described previously.<sup>8,11,23–25</sup> Areas for study were selected at random from the superficial dorsal horn at low magnification (*i.e.*, synapses not visible). Micrographs of synapses were taken at high magnification.

### Terminal Deoxynucleotidyl Transferase-mediated Deoxyuridine TUNEL and Cresyl Violet Histochemical Staining

Naive rats (n = 5) and rats that had undergone behavioral testing were deeply anesthetized and perfused transcardially with 100 ml 0.01 M phosphate-buffered saline (pH 7.4) followed by 300 ml 4% paraformaldehyde in 0.1 M phosphate buffer (pH 7.4). Lumbar enlargement segments and thymus (as a positive control) were harvested, postfixed at 4°C for 4 h, and cryoprotected in 30% sucrose overnight. Transverse sections (25  $\mu$ m) were cut on a cryostat, and two sets of sections were collected. Triphosphate nick end labeling (TUNEL) histochemical staining was carried out on one set of sections with an *in situ* cell death detection kit (Roche Molecular Biochemical, Indianapolis, IN). In brief, the sections were incubated with 20  $\mu$ g/ml proteinase K solution for 20 min at room temperature, and then with a TUNEL reaction mixture composed of terminal deoxynucleotidyl transferase at 37°C in a humidified chamber. Terminal deoxynucleotidyl transferase enzyme-incorporated fluorescein was detected with converter-alkaline phosphatase consisting of sheep anti-fluorescein antibody conjugated with phosphatase. The signal was detected using nitroblue tetrazolium chloride/5-bromo-4-chloro-3-indolyl-phosphate as color substrates. Another set of sections was stained with cresyl violet. Sections were rinsed in distilled water and incubated for 30 min in a solution of 0.2% cresyl violet (cresyl violet acetate; Sigma-Aldrich) in acetate buffer, washed in distilled water, dehydrated through a graded series of ethanol, and coverslipped.

### In Vitro Glutamate Uptake Assay

The glutamate uptake activity was measured according to a previously published method with minor modification.<sup>13,27,28</sup> In brief, animals (N = 20; formalin and saline [n = 10] *vs.* CFA and saline [n = 10]) were killed by exposure to carbon dioxide. Fresh tissue samples from the L4 and L5 spinal dorsal horns were removed as quickly as possible by laminectomy. Dorsal horns ipsilateral and contralateral to formalin or CFA injection were homogenized separately in an ice-cold buffer solution (0.5 mM EDTA, 0.5 mM EGTA, 0.2 mM phenylmethylsulfonyl fluoride, 0.32 M sucrose, 5  $\mu$ g/ml pepstatin, 5  $\mu$ g/ml aprotinin, 20  $\mu$ g/ml trypsin inhibitor, 4  $\mu$ g/ml leupeptin, 0.01 M phos-

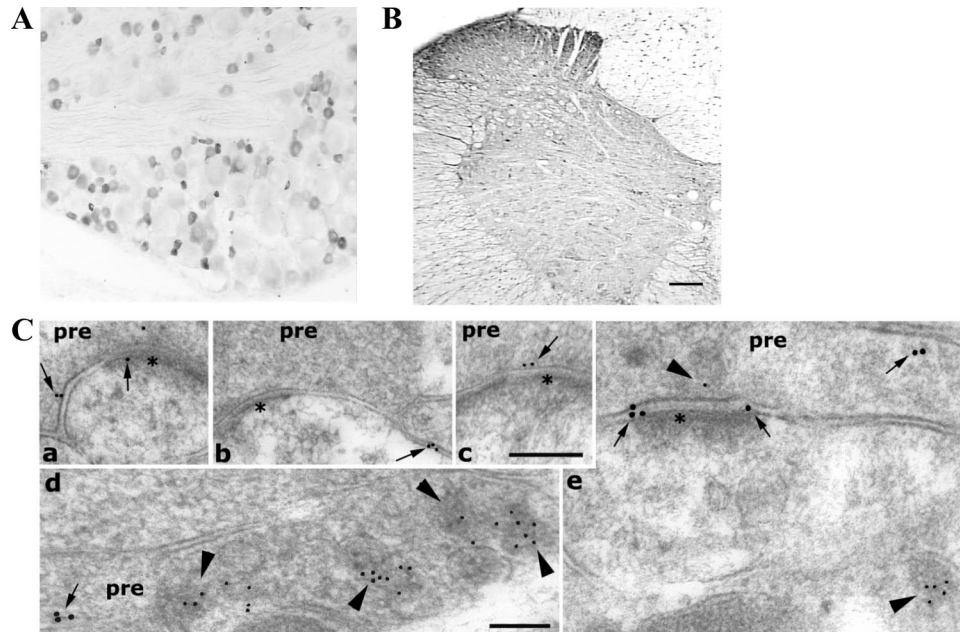


**Fig. 1.** Distribution of excitatory amino acid carrier 1 (EAAC1) in the dorsal root ganglion and spinal cord. \*Postsynaptic density. (A) EAAC1 was expressed predominantly in small dorsal root ganglion neurons. (B) EAAC1 immunoreactivity was distributed mainly in the superficial dorsal horn of the spinal cord. Scale bar, 200  $\mu\text{m}$ . (C) *a-c*: In the superficial dorsal horn, immunogold labeling for EAAC1 (arrows) was associated with postsynaptic membrane, presynaptic (pre) membrane, and the extrasynaptic membrane of the axonal terminal and postsynaptic process. Scale bar, 200 nm. *d-e*: Immunogold labeling for EAAC1 (arrows; 10 nm gold) was colocalized with that of calcitonin gene-related peptide (arrowheads; 5 nm gold), which is concentrated in dense-core vesicles in axon terminals. pre = presynaptic terminal. Scale bar, 100 nm.

phate-buffered saline). At 4°C, homogenates were centrifuged for 20 min at 1,000g. Supernatant was collected. The remaining pellets were resuspended using the same buffer solution and, at 4°C, recentrifuged for 20 min at 1,000g. The two supernatants were combined and centrifuged again at the same temperature for 10 min at 25,000g. The resulting synaptosomal pellets, which contained both neuronal and glial glutamate transporters,<sup>29,30</sup> were suspended in Krebs solutions with or without Na<sup>+</sup>. Glutamate uptake activity was determined by incubating the synaptosome preparation at 37°C for 4 min with a solution containing [<sup>3</sup>H] L-glutamate (0.4  $\mu\text{Ci}/\text{mmol}$ ; Amersham Pharmacia Biotech). The reaction was terminated by filtering synaptosomes through a Whatman GF/B filter (Maidstone, United Kingdom) presoaked in the same buffer solution. The filter was then transferred to a vial containing scintillation cocktail. Radioactivity in the final sample was measured by a liquid scintillation counter.

### Statistical Analysis

Behavioral data were statistically assessed by one-way ANOVA. Intergroup differences were analyzed by Tukey test. Western blot analysis as well as histologic and glutamate uptake data were assessed by paired Student's *t* tests to compare saline-treated (naive) and formalin- or CFA-treated groups. Locomotor data were assessed by a rank sum test. All statistical analyses were performed using a statistical software package (SigmaPlot version 8.0; Systat Software, Inc., San Jose, CA).

All statistical tests were two-tailed with a significance level of  $P < 0.05$ . Data are reported as mean  $\pm$  SE.

## Results

### Expression and Distribution of EAAC1, GLAST, and GLT-1 in the DRG and Spinal Cord

We have previously shown expression of EAAC1 mRNA and protein in DRG neurons and their central terminals.<sup>6,11</sup> Consistent with those findings, we observed EAAC1-positive cells in the DRG, mostly in small cells (fig. 1A). In the spinal cord, EAAC1 immunoreactivity was distributed predominantly in the superficial dorsal horn (fig. 1B). Under electron microscopy, immunogold labeling for EAAC1 was associated with postsynaptic membrane, presynaptic membrane, and the extrasynaptic membrane of the axonal terminals and postsynaptic dendrites in the superficial dorsal horn (fig. 1C). These synaptic contacts were asymmetrical. To further identify whether EAAC1 was localized in the primary afferent terminals, we used calcitonin gene-related peptide as a marker for nociceptive afferent terminals.<sup>31,32</sup> Double immunogold labeling revealed that EAAC1 was colocalized with calcitonin gene-related peptide in the axons and terminals in the superficial dorsal horn (fig. 1C, parts d and e). These axons and terminals contained numerous clear vesicles and a few dense core ones.

We also examined expression and distribution of GLAST and GLT-1 in the DRG and spinal cord. Reverse transcrip-

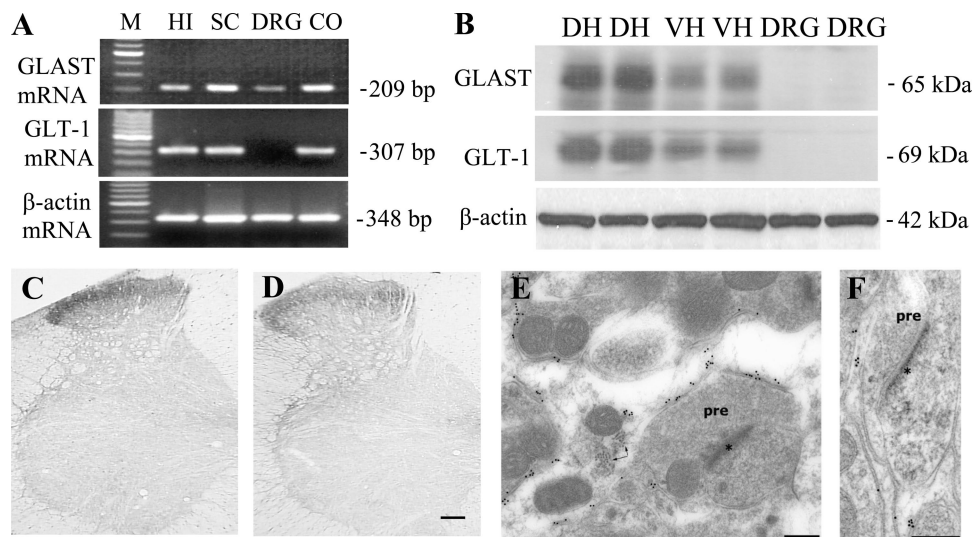


**Fig. 2.** Expression and distribution of glutamate/aspartate transporter (GLAST) and glutamate transporter-1 (GLT-1) in the dorsal root ganglion (DRG) and spinal cord (SC). (A) GLAST messenger RNA was expressed in the hippocampus (HI), SC, DRG, and cortex (CO); GLT-1 messenger RNA was expressed in HI, SC, and CO. HI and CO were used as positive controls and  $\beta$ -actin was used as a loading control. M = molecular weight standard. (B) GLAST and GLT-1 protein was expressed most abundantly in the dorsal horn (DH), much less so in the ventral horn (VH).  $\beta$ -actin was used as a loading control. In addition, GLAST (C) and GLT-1 (D) immunoreactivity was distributed predominantly in the superficial DH. Scale bar, 200  $\mu$ m. Finally, note bundles of glial filaments (small arrows) in the main shaft of the glial process in immunogold labeling of glial cells of the superficial DH for GLT-1 (E) and GLAST (F). pre = presynaptic terminal \*Postsynaptic density. Scale bar, 200 nm.

tase-PCR analysis revealed GLAST messenger RNA expression in the DRG, spinal cord, hippocampus, and cortex of adult rats, whereas GLT-1 mRNA was expressed in the spinal cord, hippocampus, and cortex, but not in the DRG (fig. 2A). PCR products of the sizes predicted from the corresponding complementary DNA sequences were detected. Nucleotide sequence analysis by automatic DNA sequencing verified that the PCR products corresponded to the complementary DNA sequences. GLAST and GLT-1 protein expression was strong in dorsal horn and weak in ventral horn but was undetectable in the DRG (fig. 2B). Consistently, immunohistochemical experiments showed GLAST and GLT-1 immunoreactivity concentrated in the superficial dorsal horn (figs. 2C and D). Under electron microscopy, immunogold labeling for GLT-1 appeared to label glia exclusively and abundantly in the superficial dorsal horn (fig. 2E). Immunogold labeling for GLAST was prominent among glial filaments and in glial membranes in the superficial dorsal horn (fig. 2F). GLT-1- and GLAST-labeled glial leaflets surround dendritic spines and the dendritic and/or axonal elements of asymmetrical axo-dendritic synapses (figs. 2E and F).

### Effects of Intrathecal Glutamate Transporter Activation and Inhibition on Inflammatory Pain

To demonstrate the role of spinal glutamate transporters in inflammatory pain, we examined the effect of intrathecal glutamate transporter activator MS-153 on formalin-induced pain behaviors during the first and second phases. MS-153 has been reported to accelerate glutamate uptake

during *in vitro* and *in vivo* studies.<sup>33–39</sup> One-way ANOVA showed that MS-153 at the doses of 10, 100, and 1,000  $\mu$ g did not significantly change the number of formalin-evoked flinches and shakes in either phase compared to that in the saline group (first phase,  $F_{3,21} = 0.21$ ,  $P = 0.89$ ; second phase,  $F_{3,21} = 0.49$ ,  $P = 0.69$ ; fig. 3A).

Next, we tested the effect of spinal glutamate transporter inhibition on formalin-induced pain behaviors. When the glutamate transporter inhibitor TBOA was given intrathecally 10 min before formalin injection, it produced a significant decrease in formalin-induced pain behaviors in the second phase ( $F_{3,36} = 7.81$ ,  $P < 0.001$ , fig. 3B), but not in the first phase ( $F_{3,36} = 1.92$ ,  $P = 0.144$ , fig. 3B). Five micrograms of TBOA reduced the number of formalin-evoked flinches and shakes by 35% ( $P = 0.02$ ), and 10  $\mu$ g reduced this number by 45% ( $P = 0.02$ ), compared to the value in the saline-treated group. A 1- $\mu$ g dose of TBOA did not influence the formalin response in either phase ( $P = 0.38$ ). We did not observe any remarkable pain behaviors on the contralateral side during formalin test. To further confirm the antinociceptive action of glutamate transporter inhibition, two other glutamate transporter inhibitors, dihydrokainate and DL-THA, were used. Similar to TBOA, dihydrokainate ( $F_{3,27} = 12.05$ ,  $P < 0.001$ , fig. 3C) and DL-THA ( $F_{3,24} = 15.22$ ,  $P < 0.001$ , fig. 3D) dramatically and dose-dependently decreased pain behaviors in the second phase of the formalin test.

We also examined the effect of spinal glutamate transporter inhibition on CFA-induced persistent inflammatory pain. Consistent with previous studies,<sup>18,19,22</sup> subcutaneous



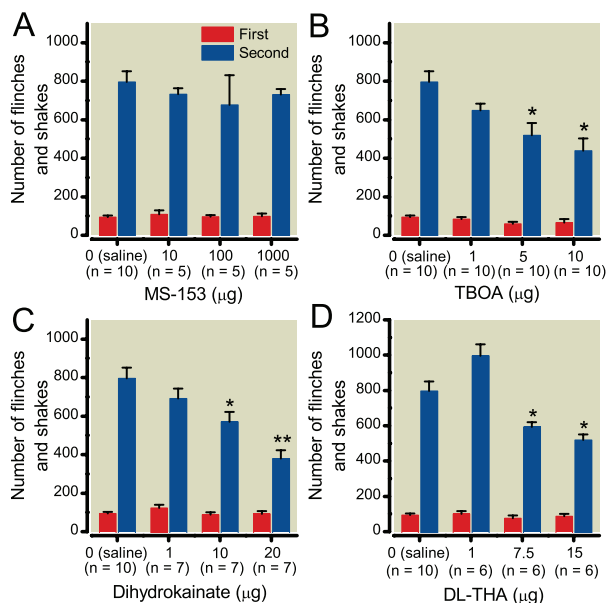


**Fig. 3.** Effects of an intrathecal glutamate transporter activator (R)-(-)-5-methyl-1-nicotinoyl-2-pyrazoline (MS-153) and inhibitors (DL-threo- $\beta$ -benzyloxyaspartate [TBOA], dihydrokainate, and DL-threo- $\beta$ -hydroxyaspartate [DL-THA]) on formalin-induced pain behaviors. Although intrathecal MS-153 did not change the number of formalin-evoked flinches and shakes in either phase of the observational session (A), intrathecal TBOA (B), dihydrokainate (C), and DL-THA (D) decreased the number of formalin-evoked flinches and shakes in the second phase significantly and in a dose-dependent manner. \* $P < 0.05$  or \*\* $P < 0.01$  versus saline (0).

injection of CFA into a hind paw induced significant thermal hyperalgesia at 6 h and 24 h postinjection in saline-treated groups on the ipsilateral side (fig. 4A). TBOA administered intrathecally significantly reduced CFA-induced thermal hyperalgesia at 6 h ( $F_{3,16} = 24.99$ ,  $P < 0.001$ , fig. 4A) and at 24 h ( $F_{3,16} = 37.68$ ,  $P < 0.001$ , fig. 4B). Compared to values observed in the saline-treated group, TBOA blocked

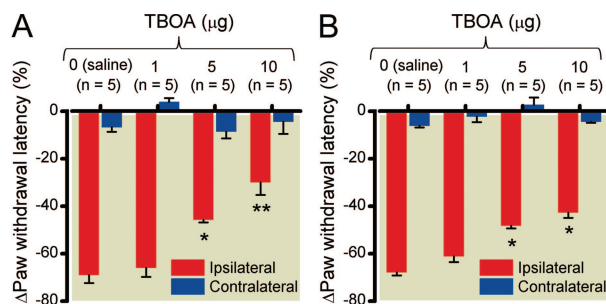


**Fig. 4.** Effect of intrathecal DL-threo- $\beta$ -benzyloxyaspartate (TBOA) on thermal hyperalgesia induced by complete Freund's adjuvant. Intrathecal TBOA significantly and dose-dependently attenuated the induced decrease in ipsilateral paw withdrawal latency at 6 (A) and 24 (B) h after injection with complete Freund's adjuvant. TBOA at the doses used (1, 5, or 10  $\mu$ g/10  $\mu$ l) did not affect basal paw withdrawal response to thermal stimulation on the contralateral side (A and B). \* $P < 0.05$  or \*\* $P < 0.01$  versus saline (0).

**Table 1.** Effect of Glutamate Transporter Inhibitors on Locomotor Functions (N = 5/group)

Treated Group	Placing	Grasping	Righting
Saline	5 (0)	5 (0)	5 (0)
DL-threo- $\beta$ -benzyloxyaspartate, 10 $\mu$ g	5 (0)	5 (0)	5 (0)
DL-threo- $\beta$ -hydroxyaspartate, 15 $\mu$ g	5 (0)	5 (0)	5 (0)
Dihydrokainate, 20 $\mu$ g	5 (0)	5 (0)	5 (0)

Data are provided as mean (standard deviation).

CFA-induced decreases in paw withdrawal latency by 34% at the 5- $\mu$ g dose ( $P = 0.03$ ) and by 57% at the 10- $\mu$ g dose ( $P = 0.009$ ) at 6 h and by 29% at the 5- $\mu$ g dose ( $P = 0.035$ ) and by 37% at the 10- $\mu$ g dose ( $P = 0.02$ ) at 24 h. A 1- $\mu$ g dose of TBOA had no effect at either time point ( $P = 0.6$  at 6 h *vs.*  $P = 0.8$  at 24 h). No dose of TBOA influenced basal paw withdrawal response to thermal stimulation on the contralateral side ( $F_{3,16} = 0.52$ ,  $P = 0.78$ , fig. 4A;  $F_{3,16} = 0.49$ ,  $P = 0.91$ , fig. 4B).

#### Effects of Intrathecal Glutamate Transporter Inhibitors on Locomotor Functions

To exclude the possibility that the antinociceptive effects of glutamate transporter inhibitors described in behavioral testing were caused by impaired motor functions, we examined the effects of TBOA, DL-THA, and dihydrokainate on locomotor functions in naive animals. As indicated in table 1, at the doses used, none of the inhibitors significantly altered placing, grasping, or righting reflexes. In addition, no significant differences were observed in the general behaviors (*e.g.*, walking and running) between the saline- and the inhibitor-treated groups.

#### Uptake Activity and Expression of Spinal Glutamate Transporters in Formalin- and CFA-induced Inflammatory Pain

To further elucidate how spinal glutamate transporter inhibition caused antinociception in inflammatory pain, we examined uptake activity and expression of spinal glutamate transporters 1 h postformalin and 6 h post-CFA. Spinal synaptosome preparations from ipsilateral and contralateral L4 and L5 dorsal horn samples were used to assess glutamate uptake activity. Saline injection did not affect basal glutamate uptake activity as compared with that of naive rats (data not shown). Analysis by paired Student's *t* test showed that glutamate uptake activity in the ipsilateral dorsal horn was decreased by 29% 1 h after formalin injection ( $t = 2.62$ ,  $P = 0.04$ , fig. 5A) and by 79% 6 h after CFA injection ( $t = 6.41$ ,  $P < 0.001$ , fig. 5B) compared with their respective controls. It is noteworthy that 6 h after CFA injection, spinal glutamate uptake activity on the contralateral side was increased by 1.5-fold compared to that of the corresponding saline

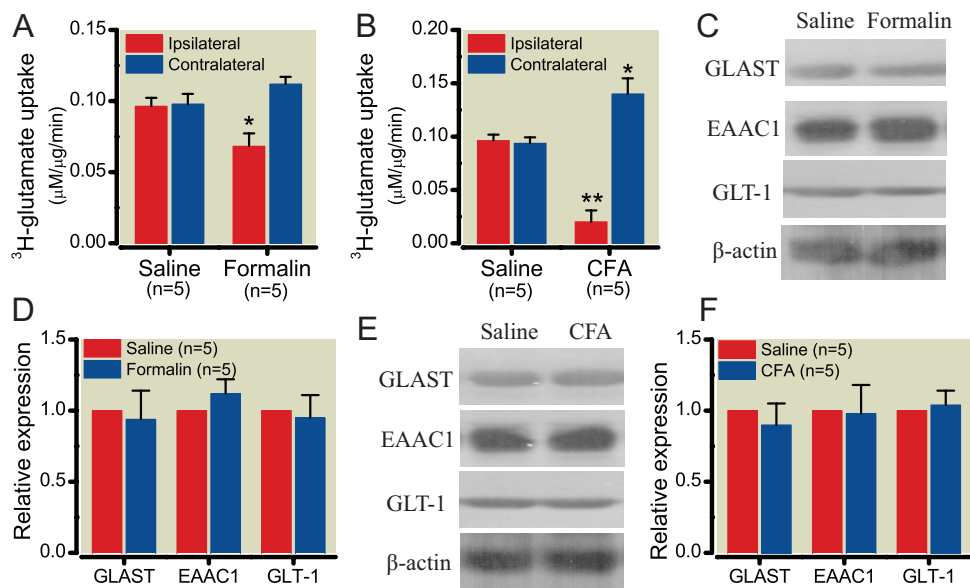


**Fig. 5.** Uptake activity and expression of glutamate transporters in the spinal cord in inflammatory pain induced by formalin and complete Freund's adjuvant (CFA) (A). Intraplantar injection of formalin significantly reduced uptake activity of dorsal horn glutamate transporters on the ipsilateral side and tended to increase activity on the contralateral side at 1 h postformalin (B). Uptake activity of dorsal horn glutamate transporters was significantly reduced on the ipsilateral side and increased on the contralateral side at 6 h after intraplantar injection of CFA. \* $P < 0.05$  or \*\* $P < 0.01$  versus saline. (C) Representative Western blots show glutamate/aspartate transporter (GLAST), excitatory amino acid carrier 1 (EAAC1), and glutamate transporter-1 (GLT-1) protein in the total soluble fraction derived from ipsilateral rat L4 and L5 dorsal horns at 1 h postsaline versus postformalin injection.  $\beta$ -actin was used as a loading control. (D) Statistical summary of densitometric analysis in figure 5C expressed relative to the corresponding saline group after normalization with the corresponding  $\beta$ -actin density. (E) Representative Western blots show GLAST, EAAC1, and GLT-1 protein in the total soluble fraction derived from ipsilateral rat L4 and L5 dorsal horns at 6 h postsaline versus post-CFA injection.  $\beta$ -actin was used as a loading control. (F) Statistical summary of densitometric analysis in figure 5E expressed relative to the corresponding saline group after normalization with the corresponding  $\beta$ -actin density.

group ( $t = 2.94$ ,  $P = 0.026$ , fig. 5B). The level of glutamate uptake activity was increased on the contralateral side 1 h after formalin injection, but the difference was not statistically significant ( $t = 1.70$ ,  $P = 0.14$ , fig. 5A). Western blot analysis showed that the amounts of total GLAST, EAAC1, and GLT-1 proteins in the ipsilateral and contralateral dorsal horn 1 h postformalin (figs. 5C and D) and 6 h post-CFA (figs. 5E and F) were similar to those in corresponding saline groups. In addition, neither formalin nor CFA injection changed basal glutamate uptake activity or EAAC1 expression in the ipsilateral L4 and L5 DRGs compared to saline treatment (data not shown).

#### Normal Morphologic Structure in Spinal Cord after Intrathecal TBOA Administration in Formalin and CFA Models

Glutamate transporter inhibition may increase extracellular glutamate concentration and produce neurotoxicity, thereby destroying the relevant dorsal horn neurons and interfering with the transmission of pain signaling. To determine whether neuronal damage was associated with intrathecal injection of glutamate transporter inhibitors during inflammatory pain, we used the TUNEL technique to examine whether 10  $\mu\text{g}/\mu\text{l}$  TBOA produced apoptosis in the spinal cord in formalin and

CFA models. We used thymus as a positive control because it normally expresses many apoptosis-positive cells.<sup>14,40</sup> Naive rats were used as negative controls.

As expected, naive rats displayed many TUNEL-positive cells in thymus (fig. 6A), but not in the spinal cord (data not shown). We did not detect any TUNEL-positive neurons in the spinal cord of rats after intrathecal administration of 10  $\mu\text{g}$  TBOA in either the formalin (fig. 6B) or CFA (fig. 6C) model. Furthermore, cresyl violet staining revealed that spinal cord neurons from TBOA-treated rats were normal, without pathologic changes, at 1 h after formalin injection and at 6 h after CFA injection (fig. 7). The number of cresyl-violet-stained cells in these two groups of rats was unchanged compared to that of naive rats (fig. 7C).

#### Effect of Blocking Group III mGluRs on the Antinociception of TBOA in Formalin and CFA Models

Group III mGluRs are expressed in primary afferent terminals in the dorsal horn.<sup>41,42</sup> Their activation reduces glutamate release from the primary afferent terminals.<sup>4,5,43</sup> To determine whether group III mGluRs participate in the antinociception caused by spinal glutamate transporter inhibition, we examined the effect of intrathecal MSOP, a group



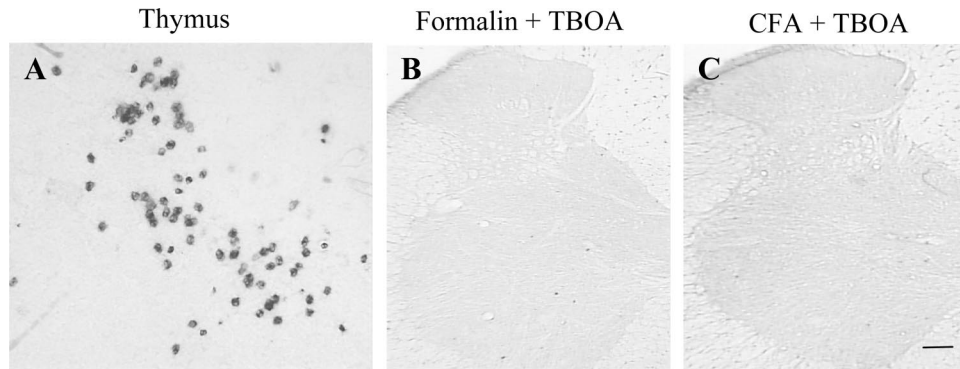


**Fig. 6.** Representative photographs show triphosphate nick end labeling–positive cells in the thymus (A), but not in the ipsilateral L4 and L5 dorsal horns of rats treated with DL-threo- $\beta$ -benzyloxyaspartate (TBOA) at 1 h postformalin injection (B) or at 6 h postinjection with complete Freund's adjuvant (CFA) (C). Scale bar, 200  $\mu$ m.

III mGluR antagonist, on TBOA-produced antinociception in the formalin and CFA models.

We found that TBOA-induced antinociceptive effects were significantly blocked by intrathecal coadministration of MSOP (second phase of formalin model:  $F_{3,16} = 30.96$ ,  $P < 0.001$ ; CFA model:  $F_{3,16} = 30.77$ ,  $P < 0.001$ ). As expected, intrathecal TBOA (10  $\mu$ g) reduced the number of formalin-induced flinches and shakes by 47% of the value in the saline-treated group in the second phase ( $P < 0.001$ , fig. 8A) and blocked the CFA-induced decrease in ipsilateral paw withdrawal latency by 60% of the value in the saline-treated group ( $P = 0.01$ , fig. 8B). The number of formalin-induced

flinches in the second phase in the group treated with MSOP and TBOA was increased by 56% ( $P = 0.04$ , fig. 8A) of the value in the TBOA-treated group. CFA-induced paw withdrawal latency in the group treated with MSOP and TBOA was decreased by 86% ( $P = 0.03$ , fig. 8B) of the value in the TBOA-treated group. MSOP (10  $\mu$ g) alone did not affect formalin-induced pain behaviors in either phase ( $P = 0.73$ , fig. 8A) or CFA-induced thermal hyperalgesia ( $P = 0.65$ , fig. 8B). It also had no effect on contralateral-side basal paw withdrawal (fig. 8B).

## Discussion

Three glutamate transporters, EAAC1, GLT-1, and GLAST, have been found in the spinal cord.<sup>6,8,11–13</sup> They are ex-

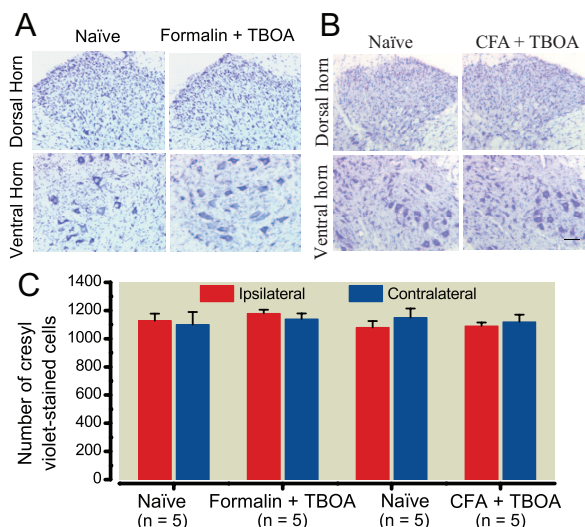


**Fig. 7.** Cresyl violet staining of spinal cord of naive rats and rats treated with DL-threo- $\beta$ -benzyloxyaspartate (TBOA) in formalin and complete Freund's adjuvant (CFA) models. (A) Representative photographs show neuronal cell architecture in dorsal and ventral horns of naive rats and rats treated with TBOA at 1 h postformalin injection. (B) Representative photographs show neuronal cell architecture in dorsal and ventral horns of naive rats and rats treated with TBOA at 6 h postinjection with CFA. (C) Average number of cresyl-violet-stained cells on the ipsilateral versus contralateral sides of spinal cord gray matter in naive rats and rats treated with TBOA at 1 h postformalin injection or 6 h post-CFA injection.

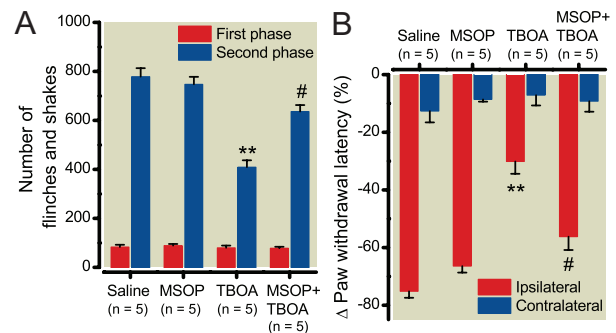


**Fig. 8.** Effect of intrathecal (RS)- $\alpha$ -methylserine-O-phosphate (MSOP), a group III metabotropic glutamate receptor antagonist, on the antinociception of intrathecal DL-threo- $\beta$ -benzyloxyaspartate (TBOA) in formalin- and complete Freund's adjuvant (CFA)-induced inflammatory pain. \*\* $P < 0.01$  versus saline. # $P < 0.01$  versus TBOA. (A) Intrathecal TBOA significantly reduced the number of formalin-evoked flinches and shakes in the second phase of the observational session. This effect was markedly blocked by coadministration of intrathecal MSOP. (B) Intrathecal TBOA significantly attenuated the CFA-induced decrease in paw withdrawal latency at 6 h post-CFA on the ipsilateral side. This effect was significantly blocked by coadministration of intrathecal MSOP. However, neither MSOP, TBOA, nor their coadministration significantly changed basal paw withdrawal response to thermal stimulation on the contralateral side.

pressed most densely in the superficial dorsal horn, which is the primary center of nociceptive processing. However, their localization and distribution at synaptic and nonsynaptic sites has not been reported. Our study provides evidence that EAAC1 is present in dorsal horn neurons and axonal terminals at both synaptic and nonsynaptic sites and in nociceptive primary afferents. In line with the current observations, we previously showed that EAAC1 colocalized with calcitonin gene-related peptide and isolectin B<sub>4</sub> in the DRG neurons and that EAAC1 immunoreactivity in the superficial dorsal horn was reduced on the side ipsilateral to the dorsal rhizotomy.<sup>11</sup> In contrast to EAAC1, GLT-1, and GLAST proteins were not detected in the DRG, although GLAST mRNA was observed in this region. Under electron microscopy, GLT-1 and GLAST were abundantly distributed in glial cells at perisynaptic sites in the superficial dorsal horn. This finding is consistent with a recent report that showed colocalization of GLT-1 and GLAST with both glial fibrillary acidic protein (a marker of astrocytes) and OX-42 (a marker of microglia) in the dorsal horn.<sup>44</sup> Thus, our findings provide a new morphologic basis for the functional role of spinal glutamate transporters in normal sensory transmission and pathologic pain (including inflammatory pain).

We and others have reported that intrathecal injection of glutamate transporter inhibitors produces hyperactivity of dorsal horn neurons, spontaneous nociceptive behaviors, and thermal and mechanical pain hypersensitivities in naive animals.<sup>14,15</sup> Based on these pronociceptive effects, it is reasonable to infer that enhancing spinal glutamate transporter uptake activity might produce antinociception in pathologic conditions. Unexpectedly, however, glutamate transporter activator MS-153<sup>33-39</sup> had no effect on formalin-induced pain behaviors, even at the highest dose (1,000  $\mu$ g). In contrast, intrathecal administration of three different glutamate transporter inhibitors, TBOA, dihydrokainate, and DL-THA, significantly blocked formalin-induced nociceptive behaviors in the second phase. Intrathecal TBOA also attenuated CFA-induced thermal hyperalgesia. Consistent with these results, Niederberger *et al.*<sup>12,17</sup> reported that pharmacologic inhibition of spinal glutamate transporter with *L-trans*-pyrrolidine-2,4-dicarboxylate or transient knock-down of GLT-1 and GLAST decreased the number of formalin-induced flinches. It is noteworthy that intrathecal administration of riluzole, a glutamate transporter activator, resulted in antinociception in rat neuropathic pain.<sup>13</sup> This controversial result might be attributed to the fact that riluzole has a number of other effects, such as blocking sodium channels, glutamate receptors, and  $\gamma$ -aminobutyric acid uptake.<sup>45</sup> In a clinical study, riluzole was ineffective against peripheral neuropathic pain.<sup>46</sup> Although dihydrokainate and DL-THA, both used in the current study, might act as agonists or antagonists at glutamate receptors, TBOA is the most potent competitive blocker of glutamate transporters and did not show any significant effects on either mGluRs or ionotropic glutamate receptors.<sup>16,35,47-49</sup> Thus, the reduced

pain-related behaviors that we observed (at least those caused by TBOA) cannot be explained by direct interaction between glutamate transporter blockers and glutamate receptors.

Here, we examined potential mechanisms by which glutamate transporter inhibitors might have antinociceptive effects on inflammatory pain. We first demonstrated that all rats treated with TBOA, DL-THA, and dihydrokainate displayed normal placing, grasping, and righting reflexes, indicating that antinociception cannot be attributed to impaired motor functions. We further found that spinal glutamate transporter uptake activity was significantly reduced on the ipsilateral side 6 h after CFA injection and 1 h after formalin injection. A similar reduction in glutamate transport activity was reported in the dorsal horn ipsilateral to peripheral nerve injury.<sup>13,50</sup> It is unclear how inflammatory and neuropathic inputs cause a reduction in spinal glutamate uptake. Although neither CFA nor formalin altered total expression of spinal glutamate transporter proteins, peripheral noxious insults might reduce plasma membrane expression of spinal glutamate transporters, a possibility that remains to be confirmed.

Reduction of spinal glutamate transporter uptake may increase glutamate concentration in the synaptic cleft and nonsynaptic extracellular space and contribute to the development and maintenance of inflammatory and neuropathic pain.<sup>6,13</sup> It is possible that, in our study, MS-153 was unable to effectively activate impaired spinal glutamate transporters to clear synaptic glutamate accumulation under inflammatory pain conditions. It is noteworthy that contralateral spinal glutamate transporter uptake activity increased to varying extents after CFA and formalin injection. The relevance of this increase is unknown but might be an attempt to compensate for the reduction in glutamate transporter uptake on the ipsilateral side to clear excess glutamate.

One might expect that, under inflammatory pain conditions, intrathecal administration of glutamate transporter inhibitors would further block clearance of glutamate and enhance the increases in synaptic and nonsynaptic extracellular glutamate in the dorsal horn. This enhancement might cause excitotoxicity, destroying susceptible dorsal horn neurons and interfering with transmission of dorsal horn nociceptive information.<sup>6</sup> However, transient treatment with TBOA did not induce any detectable spinal neuronal damage in rats subjected to the formalin or CFA model. This finding suggests that the antinociceptive effect of spinal glutamate transporter inhibition is not a result of dorsal horn neuronal excitotoxicity. It is noteworthy that we found that intrathecal coadministration of MSOP blocked the TBOA-produced antinociceptive effect in both pain models, suggesting the involvement of spinal inhibitory presynaptic group III mGluRs. Spinal group III mGluRs are activated under pathologic pain conditions, but not under normal conditions.<sup>4,5</sup> If spinal glutamate transporter inhibition enhances the activation of inhibitory presynaptic group III mGluRs, it would limit further glutamate release from primary afferents and result in an antinociceptive effect in inflammatory pain.<sup>6</sup>

This possibility is supported by a previous experiment in which inhibition of spinal glutamate uptake decreased evoked postsynaptic excitatory potentials of dorsal horn neurons in inflammatory pain—a decrease that was reversible by a group III mGluR antagonist.<sup>51</sup> Inhibition of glutamate uptake has also been reported to decrease synaptic release of glutamate.<sup>48</sup>

It is noteworthy that intrathecal MSOP did not completely reverse the antinociceptive effect of TBOA, suggesting that other potential mechanisms might exist. Glutamate transporter uptake function is dependent on the membrane potential and the transmembrane ion gradients established by the Na<sup>+</sup>-K<sup>+</sup> pump. Under inflammatory pain conditions, hyperactive dorsal horn neurons and glial cells might consume large amounts of cellular energy, disturb energy metabolism, and result in energy insufficiency.<sup>6</sup> Such insufficiency might impair the Na<sup>+</sup>-K<sup>+</sup> pump and reverse glutamate transporter operation. Indeed, during brain ischemia, glutamate transporter operation was reversed, causing glutamate release due to adenosine triphosphate depletion.<sup>49</sup> TBOA reduced glutamate release and had neuroprotective actions in brain ischemia.<sup>49</sup> We previously reported that ischemia-stimulating medium reversed the operation of glutamate transporters of dorsal horn neurons *in vitro*, causing glutamate release.<sup>52</sup> Thus, it is possible that the antinociceptive effect of glutamate transporter inhibitors might also be the result of the blockade of reversed transport and consequent release of glutamate in dorsal horn.<sup>6</sup> However, direct evidence regarding reversed operation of spinal glutamate transporters in inflammatory pain *in vivo* is lacking and remains to be further confirmed. In addition, other potential mechanisms, such as postsynaptic desensitization of dorsal horn glutamate receptors and disturbance of the glutamate-glutamine cycle in spinal glial cells might also contribute to the role of spinal glutamate transporter inhibitors in inflammatory pain.<sup>6</sup>

In summary, we have ascertained the synaptic and non-synaptic localization and distribution of EAAC1, GLT-1, and GLAST in the superficial dorsal horn. In addition, behavioral studies showed that spinal glutamate transporter inhibition produces an antinociceptive effect in formalin- and CFA-induced inflammatory pain. This effect was attenuated by a group III mGluR antagonist. Our findings suggest that spinal glutamate transporter inhibition can relieve inflammatory pain through a mechanism that involves the activation of inhibitory presynaptic group III mGluRs.

The authors thank Ya-Xian Wang, M.D. (Biologist, Laboratory of Neurochemistry, National Institute of Deafness and Other Communication Disorders, National Institutes of Health, Bethesda, Maryland), for help with immunogold experiments and Claire Levine, M.S., E.L.S. (Manager of Editorial Services, Department of Anesthesiology and Critical Care Medicine, Johns Hopkins University School of Medicine, Baltimore, Maryland), for editorial assistance.

## References

- Bennett GJ: Update on the neurophysiology of pain transmission and modulation: Focus on the NMDA-receptor. *J Pain Symptom Manage* 2000; 19:S2-6
- Danbolt NC: Glutamate uptake. *Prog Neurobiol* 2001; 65:1-105
- Yoshimura M, Jessell T: Amino acid-mediated EPSPs at primary afferent synapses with substantia gelatinosa neurones in the rat spinal cord. *J Physiol* 1990; 430:315-35
- Chen SR, Pan HL: Distinct roles of group III metabotropic glutamate receptors in control of nociception and dorsal horn neurons in normal and nerve-injured Rats. *J Pharmacol Exp Ther* 2005; 312:120-6
- Zhang HM, Chen SR, Pan HL: Effects of activation of group III metabotropic glutamate receptors on spinal synaptic transmission in a rat model of neuropathic pain. *Neuroscience* 2009; 158:875-84
- Tao Y-X, Gu J, Stephens RL Jr: Role of spinal cord glutamate transporter during normal sensory transmission and pathological pain states. *Mol Pain* 2005; 1:30
- Lehre KP, Levy LM, Ottersen OP, Storm-Mathisen J, Danbolt NC: Differential expression of two glial glutamate transporters in the rat brain: Quantitative and immunocytochemical observations. *J Neurosci* 1995; 15:1835-53
- Rothstein JD, Martin L, Levey AI, Dykes-Hoberg M, Jin L, Wu D, Nash N, Kuncl RW: Localization of neuronal and glial glutamate transporters. *Neuron* 1994; 13:713-25
- Dehnes Y, Chaudhry FA, Ullensvang K, Lehre KP, Storm-Mathisen J, Danbolt NC: The glutamate transporter EAAT4 in rat cerebellar Purkinje cells: A glutamate-gated chloride channel concentrated near the synapse in parts of the dendritic membrane facing astroglia. *J Neurosci* 1998; 18:3606-19
- Arriza JL, Eliasof S, Kavanaugh MP, Amara SG: Excitatory amino acid transporter 5, a retinal glutamate transporter coupled to a chloride conductance. *Proc Natl Acad Sci U S A* 1997; 94:4155-60
- Tao F, Liaw WJ, Zhang B, Yaster M, Rothstein JD, Johns RA, Tao YX: Evidence of neuronal excitatory amino acid carrier 1 expression in rat dorsal root ganglion neurons and their central terminals. *Neuroscience* 2004; 123:1045-51
- Niederberger E, Schmidtko A, Coste O, Marian C, Ehnert C, Geisslinger G: The glutamate transporter GLAST is involved in spinal nociceptive processing. *Biochem Biophys Res Commun* 2006; 346:393-9
- Sung B, Lim G, Mao J: Altered expression and uptake activity of spinal glutamate transporters after nerve injury contribute to the pathogenesis of neuropathic pain in rats. *J Neurosci* 2003; 23:2899-910
- Liaw WJ, Stephens RL Jr, Binns BC, Chu Y, Sepkuty JP, Johns RA, Rothstein JD, Tao YX: Spinal glutamate uptake is critical for maintaining normal sensory transmission in rat spinal cord. *Pain* 2005; 115:60-70
- Weng HR, Chen JH, Cata JP: Inhibition of glutamate uptake in the spinal cord induces hyperalgesia and increased responses of spinal dorsal horn neurons to peripheral afferent stimulation. *Neuroscience* 2006; 138:1351-60
- Minami T, Matsumura S, Okuda-Ashitaka E, Shimamoto K, Sakimura K, Mishina M, Mori H, Ito S: Characterization of the glutamatergic system for induction and maintenance of allodynia. *Brain Res* 2001; 895:178-85
- Niederberger E, Schmidtko A, Rothstein JD, Geisslinger G, Tegeder I: Modulation of spinal nociceptive processing through the glutamate transporter GLT-1. *Neuroscience* 2003; 116:81-7
- Park JS, Yaster M, Guan X, Xu JT, Shih MH, Guan Y, Raja SN, Tao YX: Role of spinal cord alpha-amino-3-hydroxy-5-methyl-4-isoxazolepropionic acid receptors in complete Freund's adjuvant-induced inflammatory pain. *Mol Pain* 2008; 4:67
- Park JS, Voitenko N, Petralia RS, Guan X, Xu JT, Steinberg JP, Takamiya K, Sotnik A, Kopach O, Haganir RL, Tao YX: Persistent inflammation induces GluR2 internalization *via*



- NMDA receptor-triggered PKC activation in dorsal horn neurons. *J Neurosci* 2009; 29:3206-19
20. Tao YX, Hassan A, Haddad E, Johns RA: Expression and action of cyclic GMP-dependent protein kinase Ialpha in inflammatory hyperalgesia in rat spinal cord. *Neuroscience* 2000; 95:525-33
  21. Tao YX, Johns RA: Activation and up-regulation of spinal cord nitric oxide receptor, soluble guanylate cyclase, after formalin injection into the rat hind paw. *Neuroscience* 2002; 112:439-46
  22. Zhang B, Tao F, Liaw WJ, Brecht DS, Johns RA, Tao YX: Effect of knock down of spinal cord PSD-93/chapsin-110 on persistent pain induced by complete Freund's adjuvant and peripheral nerve injury. *Pain* 2003; 106:187-96
  23. Furuta A, Rothstein JD, Martin LJ: Glutamate transporter protein subtypes are expressed differentially during rat CNS development. *J Neurosci* 1997; 17:8363-75
  24. He Y, Janssen WG, Rothstein JD, Morrison JH: Differential synaptic localization of the glutamate transporter EAAC1 and glutamate receptor subunit GluR2 in the rat hippocampus. *J Comp Neurol* 2000; 418:255-69
  25. Rauen T, Rothstein JD, Wässle H: Differential expression of three glutamate transporter subtypes in the rat retina. *Cell Tissue Res* 1996; 286:325-36
  26. Tao YX, Rumbaugh G, Wang GD, Petralia RS, Zhao C, Kauer FW, Tao F, Zhuo M, Wenthold RJ, Raja SN, Huganir RL, Brecht DS, Johns RA: Impaired NMDA receptor-mediated postsynaptic function and blunted NMDA receptor-dependent persistent pain in mice lacking postsynaptic density-93 protein. *J Neurosci* 2003; 23:6703-12
  27. Rothstein JD, Martin LJ, Kuncl RW: Decreased glutamate transport by the brain and spinal cord in amyotrophic lateral sclerosis. *N Engl J Med* 1992; 326:1464-8
  28. Singh OV, Yaster M, Xu JT, Guan Y, Guan X, Dharmarajan AM, Raja SN, Zeitlin PL, Tao YX: Proteome of synaptosome-associated proteins in spinal cord dorsal horn after peripheral nerve injury. *Proteomics* 2009; 9:1241-53
  29. Azbill RD, Mu X, Springer JE: Riluzole increases high-affinity glutamate uptake in rat spinal cord synaptosomes. *Brain Res* 2000; 871:175-80
  30. Mu X, Azbill RD, Springer JE: Riluzole and methylprednisolone combined treatment improves functional recovery in traumatic spinal cord injury. *J Neurotrauma* 2000; 17:773-80
  31. Carlton SM, McNeill DL, Chung K, Coggeshall RE: A light and electron microscopic level analysis of calcitonin gene-related peptide (CGRP) in the spinal cord of the primate: An immunohistochemical study. *Neurosci Lett* 1987; 82:145-50
  32. Ju G, Hökfelt T, Brodin E, Fahrenkrug J, Fischer JA, Frey P, Elde RP, Brown JC: Primary sensory neurons of the rat showing calcitonin gene-related peptide immunoreactivity and their relation to substance P, somatostatin-, galanin-, vasoactive intestinal polypeptide- and cholecystokinin-immunoreactive ganglion cells. *Cell Tissue Res* 1987; 247:417-31
  33. Abekawa T, Honda M, Ito K, Inoue T, Koyama T: Effect of MS-153 on the development of behavioral sensitization to locomotion- and ataxia-inducing effects of phencyclidine. *Psychopharmacology (Berl)* 2002; 160:122-31
  34. Abekawa T, Honda M, Ito K, Inoue T, Koyama T: Effect of MS-153 on the development of behavioral sensitization to stereotypy-inducing effect of phencyclidine. *Brain Res* 2002; 926:176-80
  35. Jabaudon D, Shimamoto K, Yasuda-Kamatani Y, Scanziani M, Gähwiler BH, Gerber U: Inhibition of uptake unmasks rapid extracellular turnover of glutamate of nonvesicular origin. *Proc Natl Acad Sci U S A* 1999; 96:8733-8
  36. Nakagawa T, Ozawa T, Shige K, Yamamoto R, Minami M, Satoh M: Inhibition of morphine tolerance and dependence by MS-153, a glutamate transporter activator. *Eur J Pharmacol* 2001; 419:39-45
  37. Nakagawa T, Fujio M, Ozawa T, Minami M, Satoh M: Effect of MS-153, a glutamate transporter activator, on the conditioned rewarding effects of morphine, methamphetamine and cocaine in mice. *Behav Brain Res* 2005; 156:233-9
  38. Shimada F, Shiga Y, Morikawa M, Kawazura H, Morikawa O, Matsuoka T, Nishizaki T, Saito N: The neuroprotective agent MS-153 stimulates glutamate uptake. *Eur J Pharmacol* 1999; 386:263-70
  39. Umemura K, Gemba T, Mizuno A, Nakashima M: Inhibitory effect of MS-153 on elevated brain glutamate level induced by rat middle cerebral artery occlusion. *Stroke* 1996; 27:1624-8
  40. Denis G, Humblet C, Verlaet M, Boniver J, Defresne MP: p53, Bax and Bcl-2 in vivo expression in the murine thymus after apoptogenic treatments. *Anticancer Res* 1998; 18:3315-21
  41. Azkue JJ, Murga M, Fernández-Capetillo O, Mateos JM, Elezgarai I, Benítez R, Osorio A, Díez J, Puente N, Bilbao A, Bidaurrezaga A, Kuhn R, Grandes P: Immunoreactivity for the group III metabotropic glutamate receptor subtype mGluR4a in the superficial laminae of the rat spinal dorsal horn. *J Comp Neurol* 2001; 430:448-57
  42. Li H, Ohishi H, Kinoshita A, Shigemoto R, Nomura S, Mizuno N: Localization of a metabotropic glutamate receptor, mGluR7, in axon terminals of presumed nociceptive, primary afferent fibers in the superficial layers of the spinal dorsal horn: An electron microscope study in the rat. *Neurosci Lett* 1997; 223:153-6
  43. Kumar N, Laferriere A, Yu JS, Poon T, Coderre TJ: Metabotropic glutamate receptors (mGluRs) regulate noxious stimulus-induced glutamate release in the spinal cord dorsal horn of rats with neuropathic and inflammatory pain. *J Neurochem* 2010; 114:281-90
  44. Xin W-J, Weng H-R, Dougherty PM: Plasticity in expression of the glutamate transporters GLT-1 and GLAST in spinal dorsal horn glial cells following partial sciatic nerve ligation. *Mol Pain* 2009; 5:15
  45. Doble A: The pharmacology and mechanism of action of riluzole. *Neurology* 1996; 47:S233-41
  46. Watase K, Hashimoto K, Kano M, Yamada K, Watanabe M, Inoue Y, Okuyama S, Sakagawa T, Ogawa S, Kawashima N, Hori S, Takimoto M, Wada K, Tanaka K: Motor discoordination and increased susceptibility to cerebellar injury in GLAST mutant mice. *Eur J Neurosci* 1998; 10:976-88
  47. Gu ZQ, Hesson DP, Pelletier JC, Maccacchini ML, Zhou LM, Skolnick P: Synthesis, resolution, and biological evaluation of the four stereoisomers of 4-methylglutamic acid: Selective probes of kainate receptors. *J Med Chem* 1995; 38:2518-20
  48. Maki R, Robinson MB, Dichter MA: The glutamate uptake inhibitor L-trans-pyrrolidine-2,4-dicarboxylate depresses excitatory synaptic transmission *via* a presynaptic mechanism in cultured hippocampal neurons. *J Neurosci* 1994; 14:6754-62
  49. Phillis JW, Ren J, O'Regan MH: Transporter reversal as a mechanism of glutamate release from the ischemic rat cerebral cortex: Studies with DL-threo-beta-benzyloxyaspartate. *Brain Res* 2000; 868:105-12
  50. Binns BC, Huang Y, Goettl VM, Hackshaw KV, Stephens RL Jr: Glutamate uptake is attenuated in spinal deep dorsal and ventral horn in the rat spinal nerve ligation model. *Brain Res* 2005; 1041:38-47
  51. Asghar AU, Bird GC, King AE: Glutamate uptake inhibition modulates dorsal horn neurotransmission: A comparison between normal and arthritic rats. *Neuroreport* 2001; 12:4061-4
  52. Chen M, Tao Y-X, Gu JG: Inward currents induced by ischemia in rat spinal cord dorsal horn neurons. *Mol Pain* 2007; 3:10